

# Entropy of city street networks linked to future spatial navigation ability

Coutrot, A.<sup>1,\*</sup>, Manley, E.<sup>2,3</sup>, Goodroe, S.<sup>4</sup>, Gahnstrom, C.<sup>4</sup>, Filomena, G.<sup>5</sup>, Yesiltepe, D.<sup>6</sup>, Dalton, R.C.<sup>6</sup>, Wiener, J. M.<sup>7</sup>, Hölscher, C.<sup>8</sup>, Hornberger, M.<sup>9</sup>, Spiers, H. J.<sup>4,\*</sup>

**1** LIRIS, CNRS, University of Lyon, France.

**2** Centre for Advanced Spatial Analysis, University College London, London, United Kingdom.

**3** School of Geography, University of Leeds, Leeds, United Kingdom.

**4** Institute of Behavioural Neuroscience, Department of Experimental Psychology, Division of Psychology and Language Sciences, University College London, London, United Kingdom.

**5** Institute for Geoinformatics, University of Münster, Münster, Germany.

**6** Department of Architecture and Built Environment, Northumbria University, Newcastle upon Tyne, United Kingdom.

**7** Department of Psychology, Ageing and Dementia Research Centre, Bournemouth University, Poole, United Kingdom.

**8** ETH Zürich, Swiss Federal Institute of Technology, Zürich, Switzerland.

**9** Norwich Medical School, University of East Anglia, Norwich, United Kingdom.

\* corresponding authors: antoine.coutrot@cnrs.fr and h.spiers@ucl.ac.uk

## Abstract

Cultural and geographical properties of the environment have been shown to deeply influence cognition and mental health<sup>1-6</sup>. While living near green spaces has been found to be strongly beneficial<sup>7-11</sup>, urban residence has been associated with a higher risk of some psychiatric disorders<sup>12-14</sup> (although see<sup>15</sup>). However, how the environment one grew up in impacts later cognitive abilities remains poorly understood. Here, we used a cognitive task embedded in a video game<sup>16</sup> to measure non-verbal spatial navigation ability in 397,162 people from 38 countries across the world. Overall, we found that people who grew up outside cities are better at navigation. More specifically, people were better at navigating in environments topologically similar to where they grew up. Growing up in cities with low Street Network Entropy (e.g. Chicago) led to better results at video game levels with a regular layout, while growing up outside cities or in cities with higher Street Network Entropy (e.g. Prague) led to better results at more entropic video game levels. This evidences the impact of the environment on human cognition on a global scale, and highlights the importance of urban design on human cognition and brain function.

## Introduction

Cognitive abilities, including spatial navigation, have been shown to correlate with specific genotypes<sup>17</sup>. However, research on brain plasticity supports the notion that experience shapes brain structure as well as function<sup>2,3</sup>. In particular, cultural and geographical properties of the environment have been shown to deeply influence cognition and mental health<sup>4,6</sup>. In rodents, exploring complex environments has a positive impact on hippocampal neurogenesis and cognition<sup>1,5</sup>. In humans, spatial navigation activates the hippocampus<sup>18</sup>, and continuous navigation of a large complex city environment increases posterior hippocampal volume<sup>19</sup>. However, how

the environment one grew up in impacts later cognitive abilities remains poorly understood for two reasons. First, human environments are manifold and much harder to characterize than a rodent’s cage. Second, collecting cognitive data of large samples from populations living in different environments is very costly<sup>20</sup>. To overcome these limitations, we measured non-verbal spatial navigation ability in 3.9 million people across all countries and examined a subset of this data (397,162 people, in 38 countries). We used a cognitive task embedded in a video game, that is predictive of real-world navigation skill<sup>16,21,22</sup>. While the task has been described previously<sup>16</sup>, we now report new data not previously published. We focused on spatial navigation due to its universal requirement across cultures, and parallels to rodent studies<sup>23,24</sup>. We quantified the complexity of participants’ environments with OSMnx, a tool giving access to the street network topology of cities anywhere in the world<sup>25</sup>. We found that, on average, people who reported having grown up in cities have worse navigation skills than those who reported growing up outside cities, even when controlling for age, gender, and level of education. This difference between city and non-city people varied across countries, being – for instance – more than 6 times larger in the USA than in Romania. To investigate these variations we computed the average Street Network Entropy (SNE) of the biggest cities of 38 countries; grid-like cities (e.g. Chicago) have a small SNE, while more organic cities (e.g. Prague) have a higher one. We found that growing up in cities with low SNE led to better performance at video game levels with a regular layout, while growing up outside cities or in cities with higher SNE led to better performance at more entropic video game levels. This confirms the impact of the environment on human cognition on a global scale, and highlights the importance of urban design on human cognition and brain function.

## Results and discussion

We used the Sea Hero Quest database, which contains the spatial navigation behaviour of 3.9 million participants measured with a mobile video game, ‘Sea Hero Quest’ (SHQ)<sup>16,22</sup>. SHQ involves navigating a boat in search of sea creatures (Figure 1). Performance of SHQ has been shown to be predictive of real-world navigation ability<sup>21</sup>. It has also allowed to differentiate high-risk preclinical Alzheimer’s disease cases from low-risk participants<sup>26</sup>. Here, we focused on the wayfinding task<sup>16</sup>, where players are initially presented with a map indicating the start location and the location of several checkpoints to find in a set order. To provide a reliable estimate of spatial navigation ability, we examined the data only from participants who had completed a minimum of eleven levels of the game, and who entered all their demographics (see Methods). This resulted in 397,162 participants from 38 countries included in our analysis, (see Supplementary Table 1 and Extended Data Fig. 1). Among them, 212,143 males (mean age:  $37.81 \pm 13.59$  years old) and 185,173 females (mean age:  $38.67 \pm 14.92$  years old).

To quantify spatial ability, we defined the “wayfinding performance” metric ( $WF$ ), which captures how efficient participants were in completing the wayfinding levels, while correcting for video-gaming skills (see Methods). We performed the same analysis for path integration levels, see Supplementary Methods and Extended Data Fig. 2. It yielded similar results. A multivariate linear regression was calculated to predict wayfinding performance based on age, gender, education and environment. Age has the strongest effect ( $F_{1,397157} = 61389$ ,  $p < 0.001$ ,  $\eta^2 = 0.127$ , Hedge’s  $g = 0.98$ , 95% CI = [0.97, 0.99]), followed by gender ( $F_{1,397157} = 20665$ ,  $p < 0.001$ ,  $\eta^2 = 0.043$ , Hedge’s  $g = 0.44$ , 95% CI = [0.43, 0.45]), education ( $F_{1,397157} = 1476.9$ ,  $p < 0.001$ ,  $\eta^2 = 0.003$ , Hedge’s  $g = 0.13$ , 95% CI = [0.13, 0.14]), and environment ( $F_{1,397157} = 1628.8$ ,  $p < 0.001$ ,  $\eta^2 = 0.003$ , Hedge’s  $g = 0.09$ , 95% CI = [0.09, 0.10]). The Hedge’s  $g$  of age is computed between participants under 25 years old (N=88,101) and above 55 years old (N=59,982). Figures 1g-h

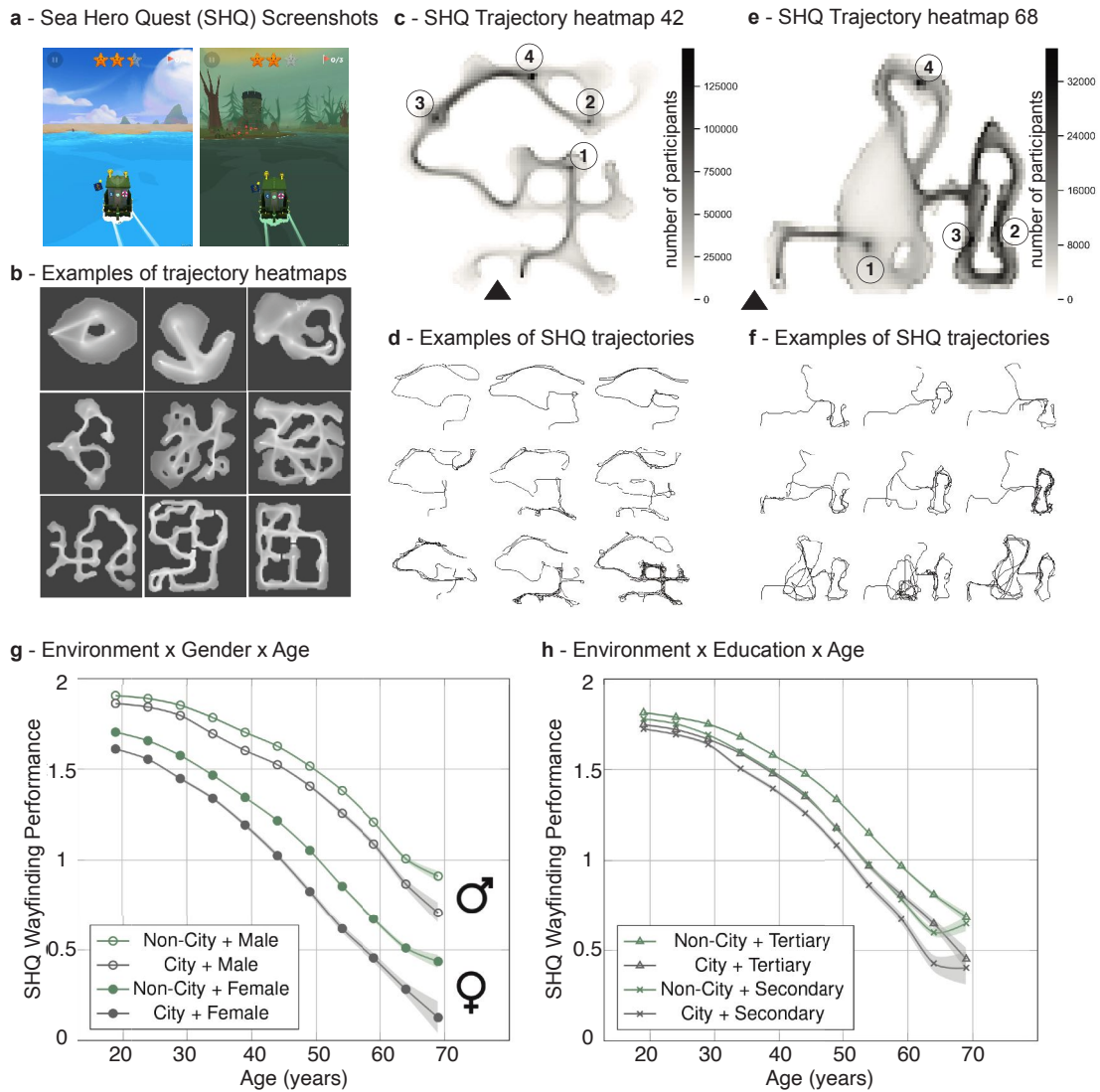
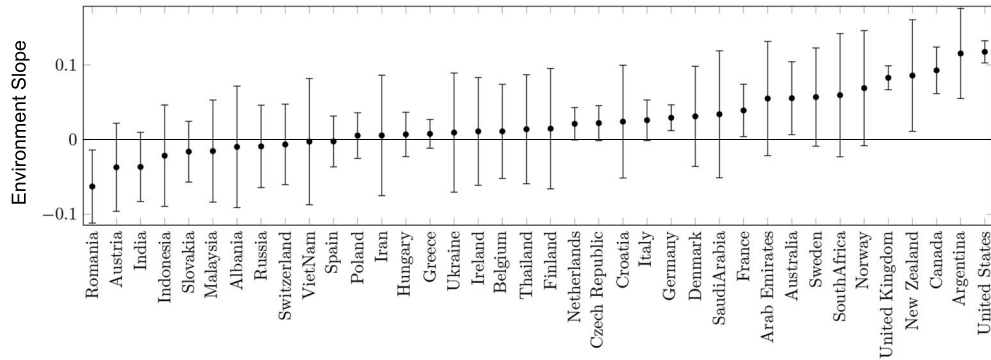


**Figure 1. | Wayfinding task** - **a** Screenshots from the game Sea Hero Quest (SHQ). See also Supplementary Video 1. **b** Nine examples of trajectory heatmaps out of the 75 SHQ levels. **c - e** Heatmaps of the trajectories of all participants in level 42 ( $n = 171,887$  participants) and level 68 ( $n = 40,251$  participants) of SHQ. The black triangle represents the starting position, and the circled numbers represent the ordered checkpoints the participants must reach. **d - f** Examples of trajectories in level 42 and 68 of SHQ. **g - h** - Association between Environment and SHQ Wayfinding Performance stratified by age, gender, and education. The SHQ Wayfinding Performance is computed from the trajectory length and has been averaged within 5-years windows. See Extended Data Fig. 7 for a breakdown of the environment classes. The error bars represent the standard errors and the center values correspond to the means.

**a - Environment effect across countries**



**b - Environment effect across cities**

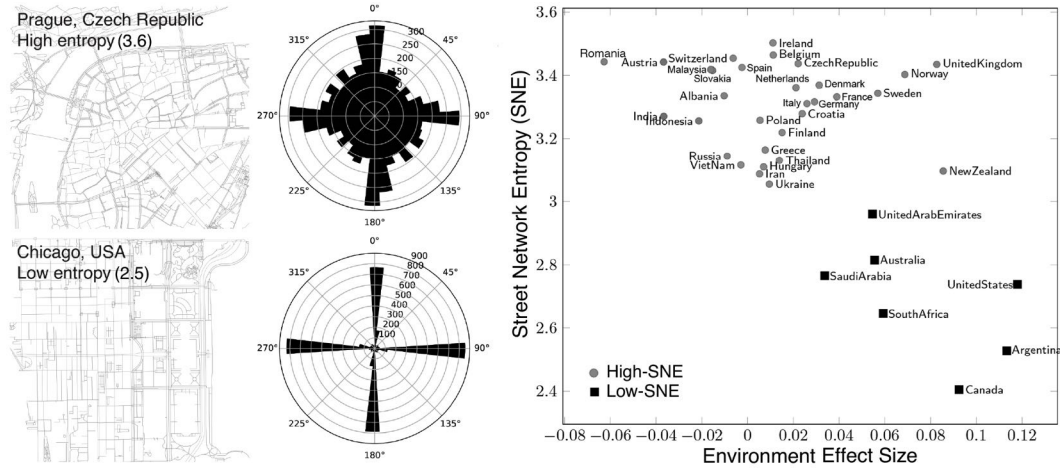


**Figure 2. | Street Network Entropy (SNE) and environment effect in 38 countries -**  
**a - Differences across countries.** We fit a linear mixed model for wayfinding performance, with fixed effects for age, gender and education, and random environment slopes clustered by country ( $n = 397,162$  participants). We plot the environment effect sizes (country slopes) for each country, with positive values indicating an advantage for participants raised outside cities. See Extended Data Fig. 1c for a world map. Error bars correspond to standard errors. **b - Left:** Two examples cities with low (Chicago, USA) and high (Prague, Czech Republic) SNE. See also Extended Data Fig. 5. Distribution of the street bearings across 36 bins of 10 degrees. **Right:** Average SNE as a function of the environment effect size (random environment slope) in each country. Positive values indicate an advantage of participants raised outside cities compared to their urban compatriots. Average SNE is the weighted average over the 10 most populated cities of the country, weighted by their population. Squares and circles correspond to the low-SNE and high SNE country groups, determined with k-means.

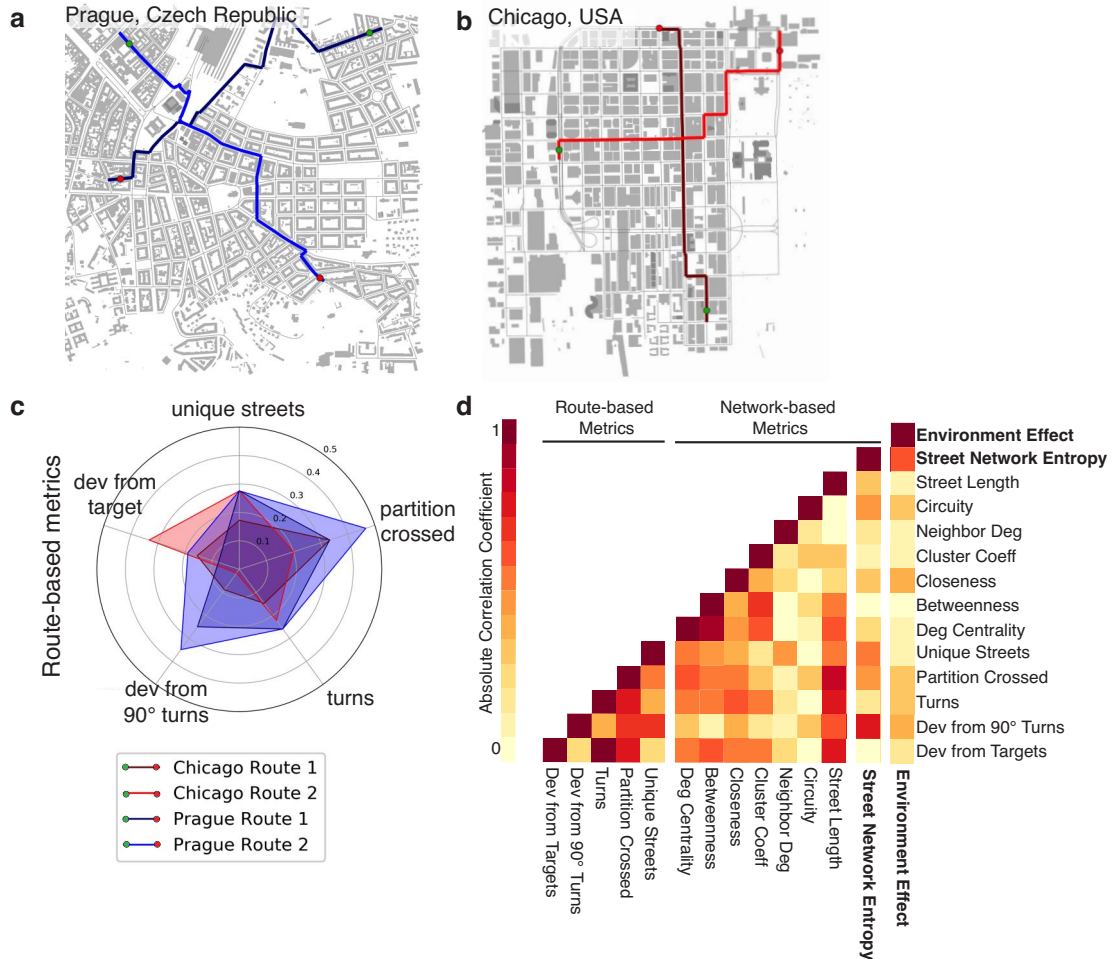


**Figure 3. | Comparison of Street Network Entropy (SNE) to other measures of city complexity measures - a - b** We simulated 1000 routes in each of the 380 included cities. Four example representative routes in two contrasting cities high/low SNE are displayed. **c** We derived five key variables from each route: Number of above 50 degree turns, Number of unique streets, Deviation from regular 90 degree turns at each turn, Overall deviation from the target and Number of transitions in the partitions in street network structure. The spider plot shows the route variables for these 4 routes, for full visualisation of the average of the 1000 routes in the 380 included cities, see Extended Data Fig. 8. We also explored a range of other graph-theoretic measures commonly considered for spatial analysis of cities. **d** Absolute correlation coefficient between all the metrics and the environment effect size. SNE is by far the metric most correlated to the environment effect size.

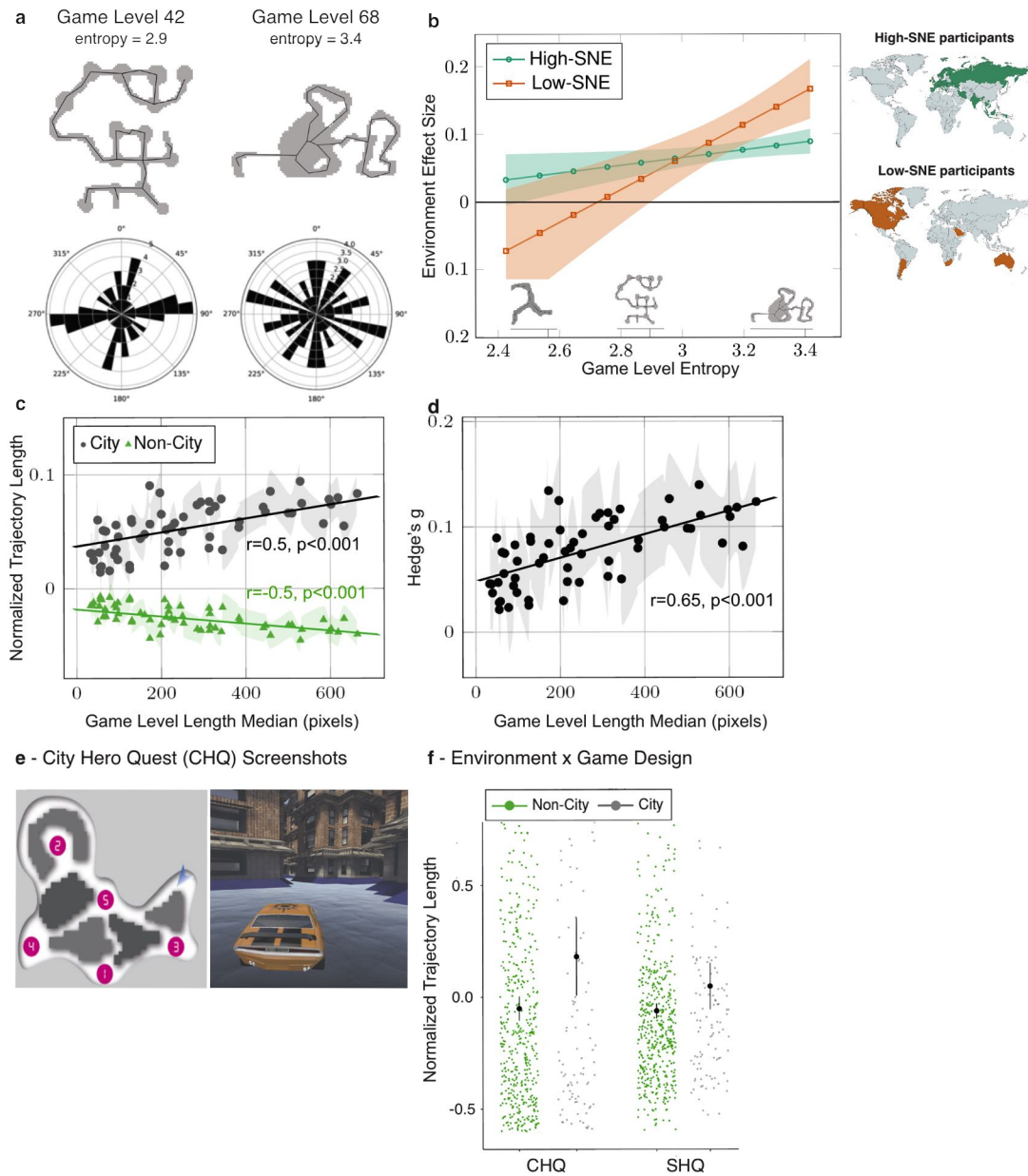


**Figure 4. | Participants are accurate at navigating more entropic game levels when they grew up in more entropic environments -** **a** The entropy of the Sea Hero Quest (SHQ) levels is computed from the bearing distribution (rose plot), shown for 2 example levels. **b** Least square regression lines of the environment effect size on game level entropy for the High-SNE and low-SNE country groups (see mini-maps and Figure 2b). We included the players that played all the SHQ wayfinding levels ( $n = 10,626$  participants). Positive values indicate an advantage of participants raised outside cities. Low-SNE environment slopes are negative for low entropy SHQ levels, suggesting that in less entropic SHQ levels, people who grew up in less entropic cities perform better than their compatriots who grew up outside cities. **c** Normalized trajectory length as a function of the level length. Trajectory lengths have been z-scored for each level. The level length is estimated by the median length over all the players. **d** For each level, the effect size of the environment on the normalized trajectory length as a function of the level length median. Positive Hedge's  $g$  corresponds to longer trajectories (i.e. worse wayfinding performance) for city participants. **e** - Screenshots from City Hero Quest (CHQ), a city-themed version of SHQ. Map and image show 1 of the 5 levels tested. **f** - Association between Environment and trajectory lengths in SHQ and CHQ ( $n = 599$  participants). The center values correspond to the means. In all panels error bars correspond to 95% confidence intervals.

represent the effect of the environment on  $WF$  stratified by age, gender, and education. We replicate previous studies showing that wayfinding performance decreases with age<sup>27,28</sup>, males perform better than females<sup>29</sup>, and performance increases with the level of education<sup>30,31</sup>. Here we now report that participants raised outside cities are more accurate navigators than city-dwellers. Having a tertiary level of education while having grown up in a city is roughly equivalent to having a secondary level of education while having grown up outside cities in terms of wayfinding performance. The sample sizes for each demographic and country are available Supplementary Table 1. Given the magnitude of the dataset, most effects are likely to always be ‘significant below the 0.001 threshold’. In the following, we will focus on effect sizes as they are independent of sample size. We computed Hedge’s  $g$  between the city and not-city groups. To marginalize the effect of age, we computed Hedge’s  $g$  within 5-years windows. Averaged over all age groups,  $g = 0.13$ , 95%CI=[0.12, 0.14], positive values corresponding to an advantage for participants who grew up outside cities. As shown in Extended Data Fig. 3, Hedge’s  $g$  remained stable across age. This stability is interesting as one could have hypothesized that the influence of the environment one grew up in could fade with age. This stability is consistent with the literature on the timing of enriched environment exposure in mice, showing that an early enriched environment exposure could provide a “reserve”-like advantage which supports an enduring preservation of spatial capabilities in older age<sup>32</sup>.

To quantify how spatial ability and environment are associated across countries, we fit a Linear Mixed Model (LMM) for wayfinding performance, with fixed effects for age, gender and education, and a random effect for country, with random slopes for environment clustered by country:  $WF_{perf} \sim age + gender + education + (1 + environment/country)$ . Figure 2a represents the environment slopes for each country, positive values indicate an advantage for participants raised outside cities, see Extended Data Fig. 1c for a world map. In terms of Hedge’s  $g$ , this spectrum ranges from Romania ( $g = -0.03$ , 95%CI=[-0.10, 0.04]) to the United States ( $g = 0.19$ , 95%CI=[0.17, 0.21]). Extended Data Fig. 4 illustrates this difference in effect size across age in different countries. For instance, while the effect size is close to being null in Germany, growing up in cities in the USA cost the equivalent of aging five years in terms of spatial ability.

To explain the variations in the association between environment and spatial ability across countries, we hypothesized that countries with lower effect sizes contain cities with more complex layouts, which places greater demands on navigation, honing the skill of those growing up in them. The impact of city topology on human spatial ability has previously been theorized in the urban design literature<sup>33,34</sup>, but the empirical studies on street networks suffer from limitations, mostly due to data availability, gathering, and processing constraints<sup>35,36</sup>, although see<sup>37</sup>. To overcome these limitations, we coupled our global dataset with the OSMnx toolbox, which provides the street network layout for anywhere in the world via OpenStreetMap<sup>25,38</sup>. Street network complexity is a manifold concept, and many metrics have been proposed to quantify it. Shannon’s information entropy<sup>39</sup> is arguably the simplest and the most general measure of network complexity, from neural to spatial networks<sup>40–43</sup>. The entropy of a variable can be interpreted as the average level of uncertainty inherent in its possible outcomes. Here, we computed the Shannon entropy of the city’s street orientations’ distribution. The smaller the entropy, the less complex - i.e. the more ordered - the city street network, see examples in Figure 2b and in Extended Data Fig. 5. Since SHQ participants only reported their home country, and not finer-grained regional information, we computed the Street Network Entropy (SNE), defined as the average of the entropy of the ten biggest cities of each country in terms of population, weighted by the city population (Supplementary Table 2). Thus, we had one SNE value per country. Figure 2b represents the SNE of countries as a function of their environment slope from

the above mixed model. The majority of the countries have a similar SNE, corresponding to the typical organic street pattern of old city cores (e.g. France, Romania, Spain, but also Thailand or India). However some other countries have distinctly smaller SNE, corresponding to the orthogonal grid, a very common planned street pattern (e.g. the United States, Argentina). The bivariate correlation between country SNE and their environment slope is significant (Pearson's  $r(36) = -0.60, p < 0.001, 95\%CI = [-0.78 -0.30]$ ). This validates our hypothesis: the lower the SNE (i.e. the simpler the street network), the worse the spatial ability of the people who grew up in cities compared to their compatriots raised outside cities. This effect remained when we control for Gross Domestic Product (GDP) per capita (linear regression predicting environment slopes, GDP per capita  $t(35)=4.02, p < 0.001$ , SNE  $t(35)=-5.86, p < 0.001$ ), see Methods. We did not find a correlation between GDP per capita and SNE ( $r(36)=0.14, p=0.40$ ), see Extended Data Fig. 6a.

While SNE captures the spatial organisation of a city, metrics based on the graph theoretic network measure topological properties of the cities, which could also play a role in shaping navigation skill. Across our 380 cities we measured the betweenness, closeness and degree centrality, average circuitry, average neighborhood degree, clustering coefficient and average street length (see Methods)<sup>43,44</sup>. After applying Bonferroni correction for multiple comparisons, we found that only circuitry (network distance/Euclidean distance) was significantly correlated with SNE ( $r(36)=0.47, p = 0.02$ ), which is coherent with<sup>43</sup>. This indicates that less regular city layouts are associated with paths across them that require more deviation around obstacles, see Figure 3. What are the mechanisms by which exposure to high SNE would lead to better navigation ability? We surmised that navigating cities with irregular street layouts would require increased demands on: 1) Keeping track of the goal direction due to greater varying street angles; 2) Spatial/prospective memory for street names and upcoming turns due the human tendency to minimise the streets/turns in an irregular laid out city<sup>45,46</sup>; 3) More hierarchical planning across neighbourhood, due to larger number of neighborhoods that might occur in irregular cities. Such demands would likely enhance the capacity of neural systems underlying orientation, prospective memory and planning abilities<sup>19,47</sup>. To empirically determine whether the specific variables we propose are linked to SNE, we employed agent-based modeling to simulate 1000 routes through each of the 380 cities to quantify: number of turns, number of streets, deviation from a 90 degree turns, overall deviation from the target and number of crossed partitions in street network (see Methods and Figure 3). After applying Bonferroni correction for multiple comparisons, we found that turns and the deviation from the goal were not significantly higher in high-SNE cities, indicating that these may not be key factors in enhancing navigation skill. Rather we found that SNE was significantly correlated with deviation from 90 degree turns ( $r(36)=0.77, p < 0.001$ ), number of streets ( $r(36)=0.57, p < 0.001$ ), and number of partitions crossed ( $r(36)=0.48, p = 0.007$ ). Thus, it appears that having to accommodate turns that deviate from 90 degrees and to navigate more streets and neighborhoods are key to enhancing navigation skill. We incorporated all network and route measures into a linear model to predict the environment effect size, and failed to find a significant equation ( $F(10,25)=1.44, p = 0.21$ ). On the other hand, when using SNE only as a predictor, a significant equation was found ( $F(1,36)=20.1, p < 0.001$ ), see Methods. This implies that it is the combination of navigational challenges that high SNE cities provide that is important for enhancing the inhabitants navigational skill.

We tested the symmetrical effect: do different SHQ level topologies interact with the effect of participant's home environment? Here our hypothesis was that people growing up in environments with more complex topologies might perform better at more elaborate, entropic SHQ levels. Conversely, people growing up in regular cities might perform better at regular SHQ levels. We used k-means to split the countries into two SNE groups, revealing a low-SNE



group and high-SNE group, see Figure 2b. We defined the SHQ level entropy as we did for the cities, with the orientations’ distribution computed from the level’s simplified Voronoi map (see Figure 4a and Methods for details). In order to include in our analysis as many level topologies as possible, we ran the following analysis on a subset of included participants who completed all SHQ levels (75 levels, 9,439 participants). We fit two LMMs for wayfinding performance: one with the participants from low-SNE countries (N=2021), the other with the participants from high-SNE countries (N=7418). Both models had fixed effects for age, gender and education, and a random effect for level, with random slopes for environment clustered by level:  $WF_{perf} \sim age + gender + education + (1 + environment/level)$ . We included all the wayfinding levels (N=42). Figure 4b represents for each level its entropy as a function of the environment slope  $s_{low}$  computed from participants in the low-SNE countries, and  $s_{high}$  computed from the high-SNE countries. Positive values correspond to an advantage of participants growing up outside cities. We observed that the only negative environment slopes correspond to low-SNE participants in less entropic levels, suggesting that people used to less entropic environments perform better in less entropic SHQ levels. The correlation coefficient was higher between the entropy of the levels and the low-SNE environment slopes (Pearson’s correlation  $r_{low} = 0.57, p < 0.001$ ) than between the entropy of the levels and the high-SNE environment slopes (Pearson’s correlation  $r_{high} = 0.44, p = 0.003$ ). This correlation slope difference did not reach statistical significance (Fisher’s  $z = 0.77, p = 0.22, 95\%$  CI for  $r_{high} - r_{low} = [-0.46, 0.20]$ ).

People living in city centres typically travel shorter distances than people living in suburbs or in more rural environments, resulting from the denser arrangement of local activity locations<sup>48,49</sup>. Thus, we hypothesized that city participants will have better wayfinding performance at SHQ levels requiring shorter trajectories. To test this hypothesis, we normalized the participants’ trajectory lengths at each level ( $M = 0, SD = 1$ ) and plotted them against the corresponding game level length median, taken over all the participants. Figure 4c shows that the performance (inversely related to the normalized trajectory lengths) of city participants decreases with the game level length median, while it increases for non-city participants. Figure 4d shows a positive correlation between the effect size (Hedge’s  $g$ ) of the environment on normalized trajectory length and the level length median (Pearson’s  $r = 0.50, p < 0.001$ ). We computed a multiple linear regression with the environment effect size as the response variable, the level entropy and trajectory length median as the predictors. We found that both entropy ( $F_{1,39} = 5.20, p = 0.02, \eta^2 = 0.12$ ) and median trajectory length ( $F_{1,39} = 13.71, p < 0.001, \eta^2 = 0.26$ ) are significant predictors of the environment effect size.

While our virtual levels varied entropy from open waters to narrow inlets (see Supplementary Video 1), the SHQ navigation task was simulated in rural settings (rivers and ocean terrain) and may potentially favor participants who reported growing up outside cities. To test this hypothesis and directly replicate the environment effect with an independent sample, we designed a city-themed version of SHQ called City Hero Quest (CHQ) and tested participants with it alongside SHQ. In CHQ, the players performed the same task as in SHQ, but driving a car in city streets, see Figure 4e and Supplementary Video 2. We collected data from new participants on 5 SHQ levels and 5 CHQ levels matched for entropy and difficulty in order to test whether our SHQ results transfer to a city context, see Extended Data Fig. 6b-d. 599 participants were recruited in the United States via the crowdsourcing platform Prolific. We chose to collect data from the US as it was the most represented country in the Prolific participant pool, and a country with a high environment effect size in the initial SHQ dataset. Sample size justification and full description of this new task are available in the Supplementary Methods. The same data analysis pipeline was applied to Sea Hero Quest and City Hero Quest data. As shown in Figure 4f, the effect size of the environment on the normalized trajectory length is similar with SHQ

data (Hedge's  $g = 0.27$ , 95%CI=[0.06, 0.47]) and CHQ data (Hedge's  $g = 0.34$ , 95%CI=[0.14, 0.54]), positive values indicating an advantage (i.e. shorter trajectories) for participants who grew up in non-city environments. The difference between the CHQ and SHQ environment effect was not significant (see Supplementary Information, CHQ Data Analysis section). This is also consistent with the effect size we found in the initial SHQ dataset when considering participants in the US on the same levels (Hedge's  $g=0.30$ , 95%CI=[0.18, 0.42]). Because participants also provided their current environment (city/non-city), we were able to show that the effect of the current environment on CHQ or SHQ performance did not reach significance (see Supplementary Information). This suggests that the childhood period is key to predicting future spatial ability.

## Conclusions

Exploring population-level cognitive performance in 38 countries, we reveal that people are better at navigating in environments topologically similar to where they grew up. We show that this association is independent of age, gender, video games skill and education. Participants who grew up in less entropic cities show better performance at less entropic game levels, while participants who grew up in more entropic cities are better at navigating more complex game levels. Similarly, participants who grew up in cities generally perform better in game levels in smaller spaces than they do in game levels in larger spaces, while participants who grew up outside cities are better in larger game levels than in game levels in smaller spaces. These results support the idea that humans develop navigation strategies aligned with the type of environment they are exposed to, which become sub-optimal in other environments (see Supplementary Discussion). It indicates that the environment one grew up in is associated with cognitive ability, and that this association is stable across the life-span. Future research will need to explore how these differences emerge during childhood through adolescence, where abrupt changes in ability can occur<sup>50</sup>.

## References

1. Kempermann, G., Kuhn, H. G. & Gage, F. H. More hippocampal neurons in adult mice living in an enriched environment. *Nature* **386**, 493–495 (1997).
2. Hackman, D. A., Farah, M. J. & Meaney, M. J. Socioeconomic status and the brain: mechanistic insights from human and animal research. *Nature Reviews Neuroscience* **11**, 651–659 (2010).
3. May, A. Experience-dependent structural plasticity in the adult human brain. *Trends in Cognitive Sciences* **15**, 475–482 (2011).
4. Van Praag, H., Kempermann, G. & Gage, F. H. Neural consequences of environmental enrichment. *Nature Reviews Neuroscience* **1**, 191–198 (2000).
5. Freund, J. *et al.* Emergence of individuality in genetically identical mice. *Science* **340**, 756–759 (2013).
6. Clemenson, G. D., Deng, W. & Gage, F. H. Environmental enrichment and neurogenesis: from mice to humans. *Current Opinion in Behavioral Sciences* **4**, 56–62 (2015).
7. Kardan, O. *et al.* Neighborhood greenspace and health in a large urban center. *Scientific Reports* **5**, 1–14 (2015).
8. Dadvand, P. *et al.* Green spaces and cognitive development in primary schoolchildren. *Proceedings of the National Academy of Sciences* **112**, 7937–7942 (2015).

9. Engemann, K. *et al.* Residential green space in childhood is associated with lower risk of psychiatric disorders from adolescence into adulthood. *Proceedings of the National Academy of Sciences* **116**, 5188–5193 (2019).
10. Berman, M. G., Stier, A. J. & Akcelik, G. N. Environmental Neuroscience. *American Psychologist* **74**, 1039–1052 (2019).
11. Bratman, G. N. *et al.* Nature and mental health: An ecosystem service perspective. *Science advances* **5**, eaax0903 (2019).
12. Lederbogen, F. *et al.* City living and urban upbringing affect neural social stress processing in humans. *Nature* **474**, 498–501 (2011).
13. Kühn, S. *et al.* In search of features that constitute an “enriched environment” in humans: Associations between geographical properties and brain structure. *Scientific Reports* **7**, 1–8 (2017).
14. Carey, I. M. *et al.* Are noise and air pollution related to the incidence of dementia? A cohort study in London, England. *BMJ Open* **8**, 1–11 (2018).
15. Stier, A. *et al.* Rethinking Depression in Cities: Evidence and Theory for Lower Rates in Larger Urban Areas. *medRxiv*. doi.org/10.1101/2020.08.20.20179036 (2020).
16. Coutrot, A. *et al.* Global Determinants of Navigation Ability. *Current Biology* **28**, 2861–2866 (2018).
17. Malanchini, M. *et al.* Evidence for a unitary structure of spatial cognition beyond general intelligence. *npj Science of Learning* **5**, 1–13 (2020).
18. Spiers, H. J. & Maguire, E. A. Thoughts, behaviour, and brain dynamics during navigation in the real world. *Neuroimage* **31**, 1826–1840 (2006).
19. Maguire, E. A., Woollett, K. & Spiers, H. J. London taxi drivers and bus drivers: a structural MRI and neuropsychological analysis. *Hippocampus* **16**, 1091–1101 (2006).
20. Xu, J. *et al.* Global urbanicity is associated with brain and behaviour in young people. *Nature Human Behaviour*, 1–15 (2021).
21. Coutrot, A. *et al.* Virtual navigation tested on a mobile app is predictive of real-world wayfinding navigation performance. *PLoS ONE* **14**, 1–15 (2019).
22. Spiers, H. J., Coutrot, A. & Hornberger, M. Explaining World-Wide Variation in Navigation Ability from Millions of People: Citizen Science Project Sea Hero Quest. *Topics in Cognitive Science* (2021).
23. Sutherland, R. J. & Hamilton, D. A. Rodent spatial navigation: at the crossroads of cognition and movement. *Neuroscience & Biobehavioral Reviews* **28**, 687–697 (2004).
24. Epstein, R. A., Patai, E. Z., Julian, J. B. & Spiers, H. J. The cognitive map in humans: spatial navigation and beyond. *Nature neuroscience* **20**, 1504 (2017).
25. Boeing, G. OSMnx: New methods for acquiring, constructing, analyzing, and visualizing complex street networks. *Computers, Environment and Urban Systems* **65**, 126–139 (2017).
26. Coughlan, G. *et al.* Toward personalized cognitive diagnostics of at-genetic-risk Alzheimer’s disease. *Proceedings of the National Academy of Sciences* **116**, 9285–9292 (2019).
27. Klencklen, G., Després, O. & Dufour, A. What do we know about aging and spatial cognition? Reviews and perspectives. *Ageing Research Reviews* **11**, 123–135 (2012).
28. Lester, A. W., Moffat, S. D., Wiener, J. M., Barnes, C. A. & Wolbers, T. The Aging Navigational System. *Neuron* **95**, 1019–1035 (2017).

29. Nazareth, A., Huang, X., Voyer, D. & Newcombe, N. A meta-analysis of sex differences in human navigation skills. *Psychonomic bulletin & review* **26**, 1503–1528 (2019).
30. Ritchie, S. J. & Tucker-Drob, E. M. How Much Does Education Improve Intelligence? A Meta-Analysis. *Psychological Science* **29**, 1358–1369 (2018).
31. Ulrich, S., Grill, E. & Flanagan, V. L. Who gets lost and why: A representative cross-sectional survey on sociodemographic and vestibular determinants of wayfinding strategies. *PLoS ONE* **14**, 1–16 (2019).
32. Fuchs, F. *et al.* Exposure to an enriched environment up to middle age allows preservation of spatial memory capabilities in old age. *Behavioural Brain Research* **299**, 1–5 (2016).
33. Lynch, K. *The Image of the City* (The Technology Press Harvard University Press, Cambridge, USA, 1960).
34. Marshall, S. *Streets and Patterns* (Spon Press, Abingdon, UK, 2005).
35. Watts, A., Ferdous, F., Diaz Moore, K. & Burns, J. M. Neighborhood integration and connectivity predict cognitive performance and decline. *Gerontology and Geriatric Medicine* **1**, 1–9 (2015).
36. Koohsari, M. J. *et al.* Cognitive Function of Elderly Persons in Japanese Neighborhoods: The Role of Street Layout. *American Journal of Alzheimers Disease Other Dementias* **34**, 381–389 (2019).
37. Bongiorno, C. *et al.* Vector-based pedestrian navigation in cities. *Nature Computational Science* **1**, 678–685 (2021).
38. Boeing, G. A multi-scale analysis of 27,000 urban street networks: Every US city, town, urbanized area, and Zillow neighborhood. *Environment and Planning B: Urban Analytics and City Science*, 1–18 (2018).
39. Shannon, C. E. A mathematical theory of communication. *Bell System Technical Journal* **27**, 379–423 (1948).
40. Barthélemy, M. Spatial Networks. *Physics Reports* **499**, 1–101 (2011).
41. Gudmundsson, A. & Mohajeri, N. Entropy and order in urban street networks. *Scientific reports* **3**, 1–8 (2013).
42. Batty, M., Morphet, R., Masucci, P. & Stanilov, K. Entropy, complexity, and spatial information. *Journal of geographical systems* **16**, 363–385 (2014).
43. Boeing, G. Urban Spatial Order: Street Network Orientation, Configuration, and Entropy. *Applied Network Science* **67**, 1–20 (2019).
44. McNamee, D., Wolpert, D. & Lengyel, M. Efficient state-space modularization for planning: theory, behavioral and neural signatures. *Advances in Neural Information Processing Systems (NIPS)*, 4511–4519 (2016).
45. Wiener, J. M., Schnee, A. & Mallot, H. A. Use and interaction of navigation strategies in regionalized environments. *Journal of Environmental Psychology* **24**, 475–493 (2004).
46. Brunyé, T. T. *et al.* Strategies for selecting routes through real-world environments: Relative topography, initial route straightness, and cardinal direction. *PloS ONE* **10**, e0124404 (2015).
47. Ekstrom, A. D., Spiers, H. J., Bohbot, V. D. & Rosenbaum, R. S. *Human spatial navigation* (Princeton University Press, 2018).

48. Salon, D. Heterogeneity in the relationship between the built environment and driving: Focus on neighborhood type and travel purpose. *Research in Transportation Economics* **52**, 34–45 (2015).
49. Lenormand, M., Bassolas, A. & Ramasco, J. J. Systematic comparison of trip distribution laws and models. *Journal of Transport Geography* **51**, 158–169 (2016).
50. Nazareth, A., Weisberg, S. M., Margulis, K. & Newcombe, N. S. Charting the development of cognitive mapping. *Journal of Experimental Child Psychology* **170**, 86–106 (2018).

## Main Text Figure legends

**Figure 1. | Wayfinding task** - **a** Screenshots from the game Sea Hero Quest (SHQ). See also Supplementary Video 1. **b** Nine examples of trajectory heatmaps out of the 75 SHQ levels. **c** - **e** Heatmaps of the trajectories of all participants in level 42 ( $n = 171,887$  participants) and level 68 ( $n = 40,251$  participants) of SHQ. The black triangle represents the starting position, and the circled numbers represent the ordered checkpoints the participants must reach. **d** - **f** Examples of trajectories in level 42 and 68 of SHQ. **g** - **h** - Association between Environment and SHQ Wayfinding Performance stratified by age, gender, and education. The SHQ Wayfinding Performance is computed from the trajectory length and has been averaged within 5-years windows. See Extended Data Fig. 7 for a breakdown of the environment classes. The error bars represent the standard errors and the center values correspond to the means.

**Figure 2. | Street Network Entropy (SNE) and environment effect in 38 countries** - **a** - Differences across countries. We fit a linear mixed model for wayfinding performance, with fixed effects for age, gender and education, and random environment slopes clustered by country ( $n = 397,162$  participants). We plot the environment effect sizes (country slopes) for each country, with positive values indicating an advantage for participants raised outside cities. See Extended Data Fig. 1c for a world map. Error bars correspond to standard errors. **b** - Left: Two example cities with low (Chicago, USA) and high (Prague, Czech Republic) SNE. See also Extended Data Fig. 5. Distribution of the street bearings across 36 bins of 10 degrees. Right: Average SNE as a function of the environment effect size (random environment slope) in each country. Positive values indicate an advantage of participants raised outside cities compared to their urban compatriots. Average SNE is the weighted average over the 10 most populated cities of the country, weighted by their population. Squares and circles correspond to the low-SNE and high SNE country groups, determined with k-means.

**Figure 3. | Comparison of Street Network Entropy (SNE) to other measures of city complexity measures** - **a** - **b** We simulated 1000 routes in each of the 380 included cities. Four example representative routes in two contrasting cities high/low SNE are displayed. **c** We derived five key variables from each route: Number of above 50 degree turns, Number of unique streets, Deviation from regular 90 degree turns at each turn, Overall deviation from the target and Number of transitions in the partitions in street network structure. The spider plot shows the route variables for these 4 routes, for full visualisation of the average of the 1000 routes in the 380 included cities, see Extended Data Fig. 8. We also explored a range of other graph-theoretic measures commonly considered for spatial analysis of cities. **d** Absolute correlation coefficient between all the metrics and the environment effect size. SNE is by far the metric most correlated to the environment effect size.

**Figure 4. | Participants are accurate at navigating more entropic game levels when they grew up in more entropic environments** - **a** The entropy of the Sea Hero Quest (SHQ) levels is computed from the bearing distribution (rose plot), shown for 2 example levels. **b** Least square regression lines of the environment effect size on game level entropy for the High-SNE and low-SNE country groups (see mini-maps and Figure 2b). We included the players that played

all the SHQ wayfinding levels ( $n = 10,626$  participants). Positive values indicate an advantage of participants raised outside cities. Low-SNE environment slopes are negative for low entropy SHQ levels, suggesting that in less entropic SHQ levels, people who grew up in less entropic cities perform better than their compatriots who grew up outside cities. **c** Normalized trajectory length as a function of the level length. Trajectory lengths have been z-scored for each level. The level length is estimated by the median length over all the players. **d** For each level, the effect size of the environment on the normalized trajectory length as a function of the level length median. Positive Hedge's  $g$  corresponds to longer trajectories (i.e. worse wayfinding performance) for city participants. **e** - Screenshots from City Hero Quest (CHQ), a city-themed version of SHQ. Map and image show 1 of the 5 levels tested. **f** - Association between Environment and trajectory lengths in SHQ and CHQ ( $n = 599$  participants). The center values correspond to the means. In all panels error bars correspond to 95% confidence intervals.

## Methods

### Data

The design and the data collection process of Sea Hero Quest have been thoroughly described in<sup>16</sup>.

**Video game** - In this study we focused on the wayfinding task. At the beginning of each wayfinding level, participants were shown locations (checkpoints) to visit on a map. The map disappeared, and they had to navigate a boat through a virtual environment to find the different checkpoints. Checkpoints were generally not encountered in the order of passage, but rather have to be navigated to by returning from one checkpoint to another (Figure 1). Participants were encouraged to collect as many 'stars' as possible across the levels: the faster the more stars were obtained. The first two levels were tutorial levels to familiarise the participant with the game commands.

**Participants** - A total of 3,881,449 participants played at least one level of the game. 60.8% of the participants provided basic demographics (age, gender, home country) and 27.6% provided more detailed demographics (home environment, level of education, see Methods). To provide a reliable estimate of spatial navigation ability, we examined the data only from participants who had completed a minimum of eleven levels of the game (including the first 4 wayfinding levels: levels 6, 7, 8 and 11) and who entered all their demographics. We removed participants above 70 years old because we previously showed a strong selection bias in this group causing their performance to be substantially higher than would be expected in unselected participants of the same age<sup>16</sup>. We also removed participants from countries with fewer than 500 players, or with education or environment levels more than 10-fold imbalanced. This resulted in 397,162 participants from 38 countries included in our analysis, (see Supplementary Table 1 and Extended Data Fig. 1).

**Demographic information** - Participants were made aware of the purpose of the game within the opening screen. Demographics were provided by consenting participants in two steps. First, their age, gender and home country were asked. Then, after having played a few levels, participants were invited to provide further information such as their level of education and the type of environment they grew up. They were asked whether they were willing to share their data with us and were guided to where they can opt out. The opt out was always available in the settings. Among the included participants there were 212,143 males (mean age:  $37.81 \pm 13.59$  years old) and 185,173 females (mean age:  $38.67 \pm 14.92$  years old). The levels ( $N =$  sample size) of education were: university ( $N=166,714$ ), college ( $N=111,463$ ), high-school ( $N=107,849$ ), and no formal ( $N=11,290$ ). We merged the university with the college levels due to their ambiguous

meaning in some countries, and the high-school with the no formal level due to the relative low sample size of the latter. Hence, in our analysis the education variable had two levels: secondary and lower (N=119,139) and tertiary (N=278,177). The levels of home environment were: city (N=109,111), suburbs (N=131,738), mixed (N=80,266), rural (N=76,047). We merged the mixed, suburb and rural levels together to facilitate the interpretation of the effect of growing-up in city (N=109,111) and non-city (N=288,051) environments. City environments are distinguished from other settings due to the higher propensity for active, self-propelled travel (e.g. walking, cycling), relative to passive, car - or public transport-based travel<sup>51</sup>, resulting from the denser arrangement of local activity locations. We furthermore anticipate that where participants have stated growing up in a city environment that there is a definitive and salient personal association with a city underlying this selection, whereas in other cases (e.g. suburban, mixed) this association is less clear, and better described as non-city. Both factors are common across international settings. Indeed, the observed clear difference between the city group and the other three groups, but little dissociation between the other three groups supports this approach, see Extended Data Fig. 7. To further validate this city / non-city dichotomy, we asked the participants to the City Hero Quest follow-up experiment the street they lived on in their home environment, and computed the entropy of the street network (SNE) in a spatial window around it (see Supplementary Methods). We then compared the SNE of people who reported having grown up in a city (N=114), suburb (N=326), rural (N=84) or mixed (N=75) environment. As shown in Extended Data Fig. 9, the SNE in cities was significantly lower than the SNE in the other environments. We ran a one-way ANOVA with the reported home environment as independent variable and the SNE as dependent variable and found a significant effect of home environment ( $F(1,3)=25.72$ ,  $p<0.001$ ). Post-hoc pairwise t-test Bonferroni-corrected for multiple comparisons showed that the SNE of a city environment was significantly lower than the SNE of all the other environments (all  $p<0.001$ ). We found no significant difference in the SNE of mixed vs rural ( $p=1$ ), suburbs vs. mixed ( $p=0.20$ ), and a small difference in the SNE of suburbs vs. rural ( $p=0.02$ ).

For the analysis on the game level entropy, we included the participants that played all the Sea Hero Quest wayfinding levels (N = 10,626). There were 5,219 males (age:  $41.89 \pm 15.95$  years old), 5,407 females (age:  $41.98 \pm 16.32$  years old), 7,429 with tertiary education, and 3,604 grew up in cities.

**Behavioural data** - We collected the trajectory of each participant across each level. The coordinates of participants' trajectories were sampled at  $F_s = 2$  Hz.

The geospatial analysis has been carried out with Python (2 and 3), while the other analyses have been done with Matlab (R2018a).

## Metrics

### Geospatial analysis

We focused on the quantification of the structural complexity of larger cities instead of the complexity of areas outside cities. This is because city streets can be more strictly compared with one another. On the opposite, areas outside cities can be heterogeneous both within and between countries, which makes the country-level averaging of their parameters problematic.

**Street Network Entropy** - We used the OSMnx Python toolbox (v.1.1.2) to download the street network topology of cities from OpenStreetMap (OSM)<sup>25</sup>. For each included city we created a street network graph from OSM data within a  $1000 \times 1000$  square meter box around the city geographical center. The use of a bounding box in the city centre is interesting as it is reflective of the wider city structure, and avoids issues related to classifications of regions, and administrative boundaries. This definition also has stronger persistence over time (considering city growth during the theoretical period of our analysis)<sup>52</sup>. To define the city geographical

centers, we used the (latitude, longitude) coordinates provided by OpenStreetMaps. Then, we computed a 36-bin edge bearings distribution (1 bin every 10 degrees), taking one value per street segment. We initially took twice as many bins as desired, then merged them in pairs to prevent bin-edge effects around common values like 0 and 90 degrees. We also moved the last bin to the front, so e.g. 0.01 degree and 359.99 degrees were binned together. We calculated the Shannon entropy of the city’s orientations’ distribution.

$$H = - \sum_{i=1}^{36} P(o_i) \log(P(o_i)) \quad (1)$$

where  $i$  indexes the bins, and  $P(o_i)$  represents the proportion of orientations that fall in the  $i^{th}$  bin<sup>43</sup>. For each of the 38 countries included in our analysis, we defined the average Street Network Entropy (SNE) as

$$SNE = \frac{1}{\sum_i \alpha_i} \sum_{i=1}^{10} \alpha_i H_i \quad (2)$$

where  $(H_i)_{i \in [1..10]}$  are the Shannon entropies of the 10 biggest cities in terms of population, and  $\alpha_i$  is the population of the  $i^{th}$  city (see Supplementary Table 1).

Since OSM mapping relies on the contributions from volunteers, we considered that this could introduce a bias, some countries being more densely mapped than others. So we compared these SNE values to the ones based on the city centers (latitude, longitude) coordinates provided by Google Maps (GM). We computed SNE value both from the drivable public streets network ('drive') and from the all non-private streets and paths network ('all'). The 'drive' network is a more reliable and consistent source of long-term street network data, given that it represents the major established roads in each city. The 'all' network, by additionally covering pathways and pedestrian zones, is more susceptible to between-country variation in volunteer mapping practices and recent planning initiatives. We found little variations, see Extended Data Fig. 10c. We also varied the size of the street network box around the city centers. If the bounding box were too big it could go beyond the city boundaries (especially for smaller cities), but if too small it might not be representative of the whole city. We computed SNEs for  $500 \times 500$ ,  $1000 \times 1000$ ,  $2000 \times 2000$  and  $5000 \times 5000$  square meter boxes. Again, our results remained stable across the different sizes, see Extended Data Fig. 10c.

#### **Graph-theoretic metrics -**

Graph based measures are calculated on the 'primal' representation of the road network for each study area, where junctions are represented by nodes and roads as edges. This representation is typical in the calculation of road network-based graph metrics. The metrics selected were chosen on the basis of their widespread use in describing street networks, and full description of their implementation can be found in<sup>25</sup>.

**Circuitry** - This measures the of the sum length of all edges divided by the sum of Euclidean distances between nodes. Thus it captures the extent of deviation required from the most direct route when moving between two points on a network<sup>53</sup>.

**Mean Cluster Coefficient** - This measure records the ratio of number of connections with neighbours over the total of number of possible connections, taken as a mean for all nodes. As such, it captures the degree close to which there is high interconnectivity between nodes in a network<sup>54</sup>.

**Mean Closeness Centrality** - Closeness represents how close a node is to all other nodes within a network. It has been demonstrated to align closely with locations of activities<sup>55</sup>



and correlated with activity in the anterior hippocampus when navigating<sup>56</sup>. The mean value for all nodes is taken.

**Mean Betweenness Centrality** - Betweenness centrality measures the extent to which a node features on shortest paths between all node pairs. Again, we use the mean value for the network, which indicates the extent to which flows of people may be spread or concentrated across the network<sup>40</sup>.

**Mean Degree Centrality** - This measure records the fraction of nodes that each node is connected to, taken as a mean for all nodes in the network. This measure reflects the extent of connectivity between nodes on a network<sup>57</sup>, is suitable for analysis interconnectivity in small areas and correlated with posterior hippocampal activity during navigation<sup>56</sup>.

**Mean Neighbor Degree** - This measures for each node the mean degree of all neighboring nodes, and reflects the degree of local node connectivity.

**Mean Street length** - This measures the mean length of street segments, and thus is an indicator of block length. This provides a measure of the density of the street network.

#### **Route-based metrics from agent-based simulations -**

All routes were calculated based on a 'dual' representation of the road network, whereby road segments are modelled as vertices and costs between vertices (e.g. distance, angular change) modelled as network edges. The Dijkstra algorithm was used for identifying the optimal paths, with road length used as the optimisation measure. For each city, 1000 routes were generated for two randomly selected origin and destination nodes (i.e. road segment centre points). For each path, the following measures were extracted.

**Unique streets** - Sum of the unique street names provided by Open Street Map encountered along the route.

**Partitions crossed** - Sum of unique partitions encountered during the route. The road network was partitioned using the Louvain community detection algorithm on the dual graph, setting edge cost as angular change. These partitions have been used a proxy for deriving perceived neighborhood boundaries<sup>58</sup>, and have demonstrated consistency with well-known regions, such as Soho and Mayfair in London, see Extended Data Fig. 5.

**Snapped angular change** - Angular deviations are calculated as the angle of incidence between two adjacent road segments, based on the connecting straight-line segments on each road polyline. The sum of absolute angular change between two consecutive road segments along a route from zero or 90 degrees (whichever is closer). We examined this novel measure because past work has shown that spatial memory for target locations is better after 90 degree or 180 rotations than other angular changes<sup>59</sup>. Memory for the angle of turns is biased towards right angles<sup>60</sup>. This suggests that it is easier to develop precise memories for low-SNE cities than for high-SNE cities. High-SNE cities would then require more training/learning, thus training navigation abilities.

**Turns** - Sum of turns between two consecutive segments surpassing 50 degrees in either direction, with more turns indicative of higher perceived cognitive distance<sup>61</sup>. We computed the same metric with 60 degrees, the results remained stable.

**Angular deviation from target** - The sum of the angular deviation from the destination, recorded at each road segment. Specifically this is recorded as the sum of differences between the angular change between two consecutive segments and the angular direction

of the target from the first segment. During navigation angular deviation from the target positively correlates with activity in the posterior parietal lobe<sup>62-64</sup>. The posterior parietal lobe is a core part of the brain regions needed for effective navigation of familiar places<sup>47</sup>.

## Video game analysis

**Wayfinding performance** - As in<sup>16</sup>, we computed the trajectory length in pixels, defined as the sum of the Euclidean distance between the points of the trajectory. To control for familiarity with technology, we normalised the trajectory lengths by dividing them by the sum of their values at the first two levels. The first two levels only reflected video gaming skill (motor dexterity with the game controls) as no sense of direction was required to complete them. We defined an overall wayfinding performance metric corrected for video gaming skill ( $WF$ ) as the 1st component of a Principal Component Analysis across the normalized trajectory lengths of the first four wayfinding levels (levels 6, 7, 8 and 11, 60.5% of variance explained). This metric being based on the trajectory length, it varies as the opposite of the performance: the longer the trajectory length, the worse the performance. We took the additive inverse of the metric and added an offset, so that  $WF = 0$  corresponds to the worst performances. Pearson’s correlation coefficient between  $WF$  and the sum of the trajectory lengths of the first two levels (video gaming skills) is weak:  $r = 0.10, p < 0.001$ , bootstrapped 95%CI = [0.09, 0.10]. The implementation of  $WF$  is available in the code presented in the *Code Availability* section.

**Game Level Entropy** - We calculated the Shannon entropy of the Sea Hero Quest level’s orientations’ distribution similarly as for the cities. To create the equivalent of ”streets” in the levels of the game, we computed the Voronoi regions from the game level’s layout, and took their edges. The Voronoi region boundaries are considered equivalent to road centre lines in the city context. We then used the Douglas-Peucker algorithm to simplify the line made of the connected segments<sup>65</sup>, see Figure 4a. For all game levels, we used a maximum offset tolerance between the original and the simplified line of three pixels. The entropy of the orientation distribution of the Game Level’s segments was then computed with equation 1.

## Statistical analysis

Further details are available in the Supplementary Information.

**Linear Mixed Model computation** - The parameters of the linear mixed models have been estimated with the maximum likelihood method (ML), and the covariance matrix of the random effects have been estimated with the Cholesky parameterization.

**Low-SNE and High-SNE country clustering** - We partitioned the 38 countries into two clusters based on their SNE with the k-means algorithm. We used the squared Euclidean distance metric. We ran the algorithm 1000 times and the arrangement never changed. The first group (low-SNE) comprised Australia, Canada, South Africa, Saudi Arabia, the United Arab Emirates, the United States of America and Argentina, with mean SNE = 2.69, SD = 0.18. The second group (High-SNE) comprised all the other countries, with mean SNE = 3.30, SD = 0.13.

**Hedge’s g** - Hedge’s g between group 1 and group 2 is defined as

$$g = \frac{(m_1 - m_2)}{s_{pooled}^*}$$

with  $m_i$  the mean of group  $i$ , and  $s_{pooled}^*$  the pooled and weighted standard deviation:

$$s_{pooled}^* = \sqrt{\frac{(n_1 - 1)s_1^2 + (n_2 - 1)s_2^2}{n_1 + n_2 - 2}}$$

with  $n_i$  the sample size of group  $i$ , and  $s_i$  the standard deviation of group  $i$ .

The 95% confidence intervals displayed in this manuscript are exact analytical confidence intervals based on iterative determination of noncentrality parameters of noncentral t or F distributions. For more details, see<sup>66</sup>.

**Confidence Intervals (CI) for Pearson's correlation coefficient** - To estimate the uncertainty around Pearson's correlation coefficient, we computed its percentile bootstrapped 95% CI. At each iteration, we resampled pairs of observations with replacement and computed their correlation values. We iterated this process 1000 times. We then sorted the correlation values and took the 2.5 and 97.5 percentiles obtained to yield a 95% CI. We illustrated this process for the correlation between Street Network Entropy and Environment effect size in Extended Data Fig. 10.

**Linear regression predicting environment effect sizes (country slopes) based on SNE and GDP per capita** - A multiple regression was calculated to predict the environment slopes based on SNE and GDP per capita. A significant equation was found ( $F(2,35)=22.40$ ,  $p < 0.001$ ) with a  $R^2 = 0.56$ : environment slopes =  $0.28 + 8.5 \times 10^{-7}(\text{GDP}) - 0.09(\text{SNE})$ . Both SNE ( $t(35)=-5.86$ ,  $p < 0.001$ ) and GDP per capita ( $t(35)=4.01$ ,  $p < 0.001$ ) were significant predictors of environment slopes.

**Modeling the environment effect with SNE vs all the other metrics** - Two linear regressions were calculated to predict the environment slopes based on

1- SNE only (model 'SNE only'): Env-slope  $\sim$  SNE

We found a significant equation ( $F(1,36)=20.1$ ,  $p < 0.001$ ), Adjusted R-Squared = 0.341, BIC = -142.11.

2- All the other metrics (model 'other metrics'): Env-slope  $\sim$  unique-streets + turns + partition-crossed + dev-from-90-turns + dev-from-targets + street-length + neighbor-degree + circuitry + clustering-coefficient + closeness-centrality + betweenness-centrality + degree-centrality.

We did not find a significant equation ( $F(10,25)=1.44$ ,  $p = 0.21$ ), adjusted R-Squared = 0.125, BIC = -105.18.

## Data Availability

A dataset with the preprocessed trajectory lengths and demographic information is available at [https://osf.io/7nqw6/?view\\_only=6af022f2a7064d4d8a7e586913a1f157](https://osf.io/7nqw6/?view_only=6af022f2a7064d4d8a7e586913a1f157)

Due to its considerable size ( $\sim 1$  To), the dataset with the full trajectories is available on a dedicated server: <https://shqdata.z6.web.core.windows.net/>. We also set up a portal where researchers can invite a targeted group of participants to play Sea Hero Quest and generate data about their spatial navigation capabilities. Those invited to play the game will be sent a unique participant key, generated by the Sea Hero Quest system according to the criteria and requirements of a specific project. <https://seaheroquest.alzheimersresearchuk.org/> Access to the portal will be granted for non commercial purposes. Future publications based on this dataset should add "Sea Hero Quest Project" as co-author.

## Code Availability

The Python and Matlab (R2018a) code allowing to reproduce the presented analyses is available along the preprocessed trajectory lengths and demographic information at [https://osf.io/7nqw6/?view\\_only=6af022f2a7064d4d8a7e586913a1f157](https://osf.io/7nqw6/?view_only=6af022f2a7064d4d8a7e586913a1f157).

## Ethics

This study has been approved by UCL Ethics Research Committee. The ethics project ID number is CPB/2013/015

## Acknowledgments

The authors wish to thank Deutsche Telekom for supporting and funding this research, Alzheimer Research UK (ARUK-DT2016-1) for funding the analysis, the Glitchers Limited for the design and game production, Saatchi and Saatchi London for project management and creative input. The geographical information used in this study has been made available by OpenStreetMap contributors under the Open Database License (<https://www.openstreetmap.org/copyright>).

## Author Contributions

HS, MH and AC supervised the project, HS, MH, AC, SG, CG, RD, JW, and CH designed research; AC, EM, GF, and DY analyzed data; AC, EM and HS wrote the paper.

## Declaration of Interests

The authors declare no competing interests.

## Material and Correspondence

Correspondence and material requests should be addressed to Dr Coutrot ([antoine.coutrot@cnrs.fr](mailto:antoine.coutrot@cnrs.fr)) or Prof Hugo Spiers ([h.spiers@ucl.ac.uk](mailto:h.spiers@ucl.ac.uk)).

## Extended Data Figure legends

**Extended Data Fig. 1. | Color-coded world maps. a** - Sample size. **b** - Proportion of city participants. **c** - Environment effect size computed from a Linear Mixed Model predicting Wayfinding Performance, with fixed effects for age, gender and education, and random environment slopes clustered by country. The environment effect sizes are the environment slopes clustered by country, identical to the values in Figure 2a.

**Extended Data Fig. 2. | Association between age, home environment, country, and Path Integration Performance. a** - Path Integration Performance as a function of age for male and female participants who grew up in city and non-city environments. Path Integration Performance is averaged within 5-year windows, center values correspond to the means. **b** - Difference of the effect of growing up outside cities on Path Integration Performance across countries. We fit a logistic mixed model for Path Integration Performance, with fixed effects for age, gender and education, and random environment slopes clustered by country, see Supplementary Methods. Positive values indicate an advantage for participants raised outside cities. **c** - Street Network Entropy (SNE) as a function of the environment effect size (random environment slope) in each country, as in Figure 2b, see Supplementary Methods. All error bars correspond to standard errors,  $n = 182,122$  participants.

**Extended Data Fig. 3. | Environment effect size across age, gender (top) and level of education (bottom).** Effect size is quantified with Hedge's  $g$ , within 5-year windows. Positive values correspond to an advantage for participants who grew-up outside cities. Error bars correspond to 95% confidence intervals and the center values correspond to the means.

**Extended Data Fig. 4. | Wayfinding Performance in city and non-city environments**

**across age, in each country.** Wayfinding Performance is averaged within 10-year windows. Error bars correspond to standard errors and center values correspond to the means. Note that these values correspond to raw Wayfinding Performance, i.e. they have not been corrected for age, gender or education. Note: VietNam and Albania y axis lower bound is 0 to allow display of data points, instead of 0.5 for the rest of the countries. Altogether, we included  $n = 397,162$  participants.

**Extended Data Fig. 5. | Examples of city street networks - a** - The road networks of New York City (USA, right) and London (UK, left) have been partitioned using the Louvain community detection algorithm on the dual graph, setting edge cost as angular change. The road networks within a  $3 \times 3 \text{ km}^2$  box around the city centres are represented. **b** - Street network of the 10 biggest cities in terms of population in Argentina and in Romania. We used OSMnx to gather the “drive” Open Street Map network within  $1000 \times 1000 \text{ m}^2$  boxes around each city centre. The reasons behind these differences are mostly historical. In South America, grid city design is characteristic of Hispanic American colonization, while disorganized street networks correspond to the typical organic street pattern of old European city cores.

**Extended Data Fig. 6. | a** - Gross Domestic Product (GDP) per capita as a function of Street Network Entropy. **b** - Screenshot from Sea Hero Quest (SHQ, left) and City Hero Quest (CHQ, right). **c** - Subset of SHQ levels used in the second experiment run on Prolific. **d** - CHQ levels used in the second experiment.

**Extended Data Fig. 7. | Association between age, home environment, country, and Wayfinding Performance. a** - Wayfinding Performance as a function of age for participants who grew up in city, suburb, mixed and rural environments. Data points correspond to the wayfinding performance averaged within 5-year windows. **b** - Difference in the effect of growing up outside cities on wayfinding performance across countries. We fit a linear mixed model for wayfinding performance, with fixed effects for age, gender and education, and random environment slopes clustered by country, as in Figure 2a. Suburbs, Mixed and Rural environment slopes are represented, with City environment as baseline. Positive values correspond to an advantage compared to growing up in cities. Countries are ranked according to their suburb slope. The slopes of the different non-city environments are highly correlated: Pearson’s  $r(\text{suburb, mixed}) = 0.97, p < 0.001$ ,  $r(\text{suburb, rural}) = 0.72, p < 0.001$ ,  $r(\text{mixed, rural}) = 0.53, p < 0.001$ . The country ranking is very similar to the one with only 2 classes (city / non-city): Spearman’s  $r(\text{non-city, suburb}) = 0.85, p < 0.001$ ,  $r(\text{non-city, mixed}) = 0.73, p < 0.001$ ,  $r(\text{non-city, rural}) = 0.94, p < 0.001$ . P-values are from a t-test testing the hypothesis of no correlation against the alternative hypothesis of a nonzero correlation. **c** - Pairwise differences between random environment slopes shown in panel b, averaged over countries. We show that the average difference in effect size between the city environment and the other 3 environments (city-rural, city-mixed, city-suburb) are around 10 times larger than the difference between the ‘non-city’ environments (rural-mixed, mixed-suburb, rural-suburb). This supports the approach to cluster together rural, mixed and suburb environments. All error bars correspond to standard errors,  $n = 397,162$  participants.

**Extended Data Fig. 8. | Environment effect size and city complexity measures in high-SNE and low-SNE countries** - In each of the 380 included cities we computed a range of metrics to quantify different aspects of its complexity. We then took an average of these metrics weighted by the city population to have one value per country. We normalized these values by dividing them by their maximum. **Network-based metrics** - On top of the Street Network Entropy used in this study, we computed other graph-theoretic measures commonly considered for spatial analysis of cities: average street length, circuitry, neighborhood degree, clustering coefficient, closeness centrality, betweenness centrality, and degree centrality. **Route-based metrics** - we simulated 1000 routes in each city, and quantified five key variables derived from

each route: number of unique streets, number of transitions in the partitions in street network structure, deviation from regular 90 degree turns at each turn, overall deviation from the target and number of turns above 50 degrees. Individual data points correspond to countries (n=38). In the boxplots, the horizontal bar represents the sample median, the hinges represent the first and third quartiles, and the whiskers extend from the hinges to the largest/lowest value no further than  $\pm 1.5 * \text{IQR}$  from the hinge (where IQR is the inter-quartile range).

**Extended Data Fig. 9. | Street Network Entropy across reported home environments.** SNE computed at the home addresses of the 599 participants to the follow-up experiment City Hero Quest as a function of the reported type of home environment. The size of the square boxes used to compute the SNE were adjusted for the average street density within each reported environment (see Supplementary Methods). Error bars correspond to standard errors and center values correspond to the means.

**Extended Data Fig. 10. | Estimation of the robustness of the Pearson’s correlation between Street Network Entropy (SNE) and environment effect size.** Bootstrapped correlation coefficients computed from 1000 resampling with replacement. **a** - Histogram of the computed correlation coefficients. We obtained  $r = -0.60$ , 95% CI =  $[-0.78 -0.30]$ . **b** - Regression lines for each sample. **c** - Pearson’s correlation between environment effect size and different SNE calculations. The SNE set in bold is the one used in this manuscript. OSM = OpenStreetMaps, GM = Google Maps. P-values are from a t-test testing the hypothesis of no correlation against the alternative hypothesis of a nonzero correlation.

## Supplementary Video legends

**Supplementary Video 1** | Examples of navigation in two Sea Hero Quest levels: level 27 (left) and level 58 (right).

**Supplementary Video 2** | Example of navigation in one City Hero Quest level.

## References

51. Montello, D. R. *A conceptual model of the cognitive processing of environmental distance information* in *International Conference on Spatial Information Theory* (2009), 1–17.
52. Masucci, A. P., Arcaute, E., Hatna, E., Stanilov, K. & Batty, M. On the problem of boundaries and scaling for urban street networks. *Journal of the Royal Society Interface* **12** (2015).
53. Giacomini, D. J. & Levinson, D. M. Road network circuitry in metropolitan areas. *Environment and Planning B: Planning and Design* **42**, 1040–1053 (2015).
54. Jiang, B. & Claramunt, C. Topological analysis of urban street networks. *Environment and Planning B: Planning and Design* **31**, 151–162 (2004).
55. Porta, S. *et al.* Street centrality and densities of retail and services in Bologna, Italy. *Environment and Planning B: Planning and Design* **36**, 450–465 (2009).
56. Javadi, A.-H. *et al.* Hippocampal and prefrontal processing of network topology to simulate the future. *Nature Communications* **8**, 1–11 (2017).
57. Jiang, B. & Claramunt, C. A structural approach to the model generalization of an urban street network. *GeoInformatica* **8**, 157–171 (2004).
58. Filomena, G., Verstegen, J. A. & Manley, E. A computational approach to ‘The Image of the City’. *Cities* **89**, 14–25 (2019).

59. Mou, W., McNamara, T. P., Valiquette, C. M. & Rump, B. Allocentric and egocentric updating of spatial memories. *Journal of experimental psychology: Learning, Memory, and Cognition* **30**, 142 (2004).
60. Tversky, B. Distortions in memory for maps. *Cognitive Psychology* **13**, 407–433 (1981).
61. Sadalla, E. K. & Magel, S. G. The perception of traversed distance. *Environment and Behavior* **12**, 65–79 (1980).
62. Spiers, H. J. & Maguire, E. A. A navigational guidance system in the human brain. *Hippocampus* **17**, 618–626 (2007).
63. Howard, L. R. *et al.* The hippocampus and entorhinal cortex encode the path and Euclidean distances to goals during navigation. *Current Biology* **24**, 1331–1340 (2014).
64. Spiers, H. J. & Barry, C. Neural systems supporting navigation. *Current Opinion in Behavioral Sciences* **1**, 47–55 (2015).
65. Douglas, D. H. & Peucker, T. K. Algorithms for the reduction of the number of points required to represent a digitized line or its caricature. *Cartographica: the international journal for geographic information and geovisualization* **10**, 112–122 (1973).
66. Hentschke, H. & Stüttgen, M. C. Computation of measures of effect size for neuroscience data sets. *European Journal of Neuroscience* **34**, 1887–1894 (2011).